

UNCLASSIFIED

AD NUMBER

AD030930

CLASSIFICATION CHANGES

TO: unclassified

FROM: confidential

LIMITATION CHANGES

TO:  
Approved for public release; distribution is unlimited.

FROM:  
Distribution authorized to DoD only;  
Administrative/Operational Use; 30 DEC 1953.  
Other requests shall be referred to Bureau of  
Aeronautics, Department of the Navy,  
Washington, DC 20350. Pre-dates formal DoD  
distribution statements. Treat as DoD only.

AUTHORITY

BUWEPS ltr dtd 16 Mar 1965; BUWEPS ltr dtd 16  
Mar 1965

THIS PAGE IS UNCLASSIFIED

R  
M  
I

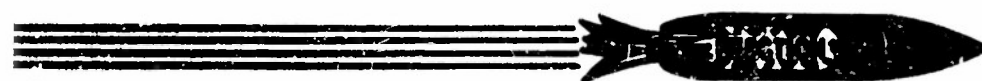
**CONFIDENTIAL**

Contract NGas 53-406-c  
Report RMI - 487 - F  
December 30, 1953

**Combustion Kinetics  
Investigation**

**FINAL REPORT**

REACTION MO TO RES INC  
ROCKAWAY NEW JERSEY



**CONFIDENTIAL**

54AA-22296

NOTICE: THIS DOCUMENT CONTAINS INFORMATION AFFECTING THE NATIONAL DEFENSE OF THE UNITED STATES WITHIN THE MEANING OF THE ESPIONAGE LAWS, TITLE 18, U.S.C., SECTIONS 793 and 794. THE TRANSMISSION OR THE REVELATION OF ITS CONTENTS IN ANY MANNER TO AN UNAUTHORIZED PERSON IS PROHIBITED BY LAW.

*Reproduced*  
FROM LOW CONTRAST COPY.

**CONFIDENTIAL**

Report RMI-487-F

No. of Pages 32

Copy No. 60

REACTION MOTORS, INC.  
COMBUSTION KINETICS INVESTIGATION

T. Raines  
J. Pisani

Final Report

Contract NOas 53-406-c

RMI Project 487

SUBMITTED BY:

*Louis R. Rapp*  
LOUIS R. RAPP  
Chief Chemist

APPROVED BY:

*R. L. Wehrli*  
R. L. WEHRLI  
Chief of Research

APPROVED BY:

*H. B. Horne*  
H. B. HORNE  
Manager of Research  
and Engineering

**CONFIDENTIAL**

REACTION MOTORS, INC.  
ROCKAWAY, NEW JERSEY

TABLE OF CONTENTS

	Page No.
LIST OF ILLUSTRATIONS	v
LIST OF TABLES	ix
1. SUMMARY	1
2. INTRODUCTION	2
3. FLAME SPEED MEASUREMENTS	3
3.1 Apparatus	3
3.2 Operational Procedure	5
3.3 Analysis of Data	6
3.4 Discussion of Data	6
4. SLOW OXIDATION STUDIES	8
4.1 Apparatus	8
4.2 Operational Procedure	9
4.3 Analysis of Data	9
4.4 Discussion of Data	11
5. ROCKET MOTOR INVESTIGATION	13
5.1 Apparatus	13
5.2 Operational Procedure	16
5.3 Analysis of Data	17
5.4 Discussion of Data	17
6. CORRELATION OF DATA	26
7. CONCLUSIONS	29
8. RECOMMENDATIONS	30
REFERENCES	31
APPENDIX A - Theoretical Performance Parameters for Various Fuel-Liquid Oxygen Systems at a Chamber Pressure of 300 psia and at an Exhaust Pressure of 1 Atmosphere. Frozen Equilibrium Method.	32

LIST OF ILLUSTRATIONS

<u>Figure No.</u>	<u>Title</u>	<u>Page No.</u>
1.	Flame Speed Apparatus - Schematic	3
2.	Electronic and Photocell Wiring Diagram - Schematic	4
3.	Recorded Oscillogram of an Ethane-Air Flame	5
4.	Apparent Flame Speed vs Percent Fuel in Mixture	7
5.	Slow Oxidation Flow Apparatus - Schematic	8
6.	Percent CO <sub>2</sub> Evolved vs Contact Time	11
7.	Variable-Positioning-Injector for Eleven Pound Thrust Chamber	14
8.	Eleven Pound Thrust Chamber With A Variable Position Injector	15
9.	The Portable Test Stand - Schematic	15
10.	Eleven Pound Thrust Motor Unit and Stand	16
11.	Instrument Control Panel for Eleven Pound Thrust	16
12.	Characteristic Velocity vs Mixture Ratio, Ethylene-Liquid Oxygen	21
13.	Characteristic Velocity vs Mixture Ratio, Cyclopropane-Liquid Oxygen	21
14.	Characteristic Velocity vs Mixture Ratio, Ammonia-Liquid Oxygen	22
15.	Characteristic Velocity vs Mixture Ratio, Ethylene Oxide-Liquid Oxygen	22
16.	Maximum C* Obtained Experimentally vs Chamber Length	23
17.	Theoretical C* vs Mixture Ratio	24

LIST OF ILLUSTRATIONS (cont'd)

<u>Figure No.</u>	<u>Title</u>	<u>Page No.</u>
18.	Percent Theoretical Maximum C* Obtained Experimentally vs Chamber Length	25
19.	Maximum Apparent Flame Speed vs $\frac{1}{m}$	27
20.	Relationship Among Chamber Volume, Flow Rate, and $\frac{1}{m}$	28

LIST OF TABLES

<u>Table No.</u>	<u>Title</u>	<u>Page No.</u>
1.	Apparent Flame Speed Data	7
2.	Slow Oxidation Data	10
3.	Experimental C* At Various Chamber Lengths, Ethylene-Liquid Oxygen	18
4.	Experimental C* At Various Chamber Lengths, Cyclopropane-Liquid Oxygen	18
5.	Experimental C* At Various Chamber Lengths, Ammonia-Liquid Oxygen	19
6.	Experimental C* At Various Chamber Lengths, Ethylene Oxide - Liquid Oxygen	20
7.	Summary of Data	26

## 1. SUMMARY

The apparatus and operational procedure for the flame speed, slow oxidation, and small scale rocket motor studies are discussed. In order to correlate the data obtained under the previous contract with the data obtained under this contract, essentially the same type of equipment and methods were used for all operations in both contracts.

The apparent flame speeds for a mixture of ethylene, of cyclopropane, and of ethylene oxide with air at an ambient temperature of 81°C are reported. The maximum apparent flame speeds were found to be as follows: for ethylene, 169 cm/sec; for cyclopropane, 109 cm/sec; and for ethylene oxide, 266 cm/sec.

The results of slow oxidation studies of ethylene, cyclopropane, and ethylene oxide with oxygen as an oxidizer at O/F by weight ratios corresponding to maximum experimental characteristic velocity  $C^*$  values are reported. The cyclopropane-oxygen system did not yield a measurable amount of  $CO_2$  under the conditions of the experiment. A straight line from the plot of percent  $CO_2$  versus the logarithm of the contact time is obtained in the case of ethylene but not in the case of ethylene oxide. The percent  $CO_2$  from the latter decreases with increasing contact time. An equation for the ethylene curve is presented and the induction period for the formation of  $CO_2$  determined by linear extrapolation turned out to be 79 sec.

Characteristic velocity measurements as a function of the O/F ratio and chamber length were determined in an 11-pound-thrust motor for the ethylene, cyclopropane, ethylene oxide, and ammonia systems with liquid oxygen as oxidizer. The results are presented in tabular and graphical form. The respective maximum characteristic exhaust velocity values in ft/sec for the ethylene-lox, cyclopropane-lox, ammonia-lox, and ethylene oxide-lox systems were found to be: 6510 (O/F = 2.27, 4 in. chamber length), 5530 (O/F = 2.05, 5 in. chamber), 5310 (O/F = 1.40, 6 in. chamber), and 5520 (O/F = 1.60, 7 in. chamber). The theoretical  $C^*$  values for these systems are also tabulated and graphed.

Although the slow oxidation data yield a straight line for the percent of  $CO_2$  evolved vs the logarithm of the contact time for the ethylene-oxygen system at 350°C, the results do not substantiate the relationships proposed in Ref. 1. Furthermore, the facts that the cyclopropane-oxygen system did not yield a measurable amount of  $CO_2$  at 350°C and that ethylene oxide did not yield a straight line in the slow oxidation plot cast grave doubt on the general validity of the proposed relationships among flame speed, slow oxidation, and small scale rocket motor characteristics data.

2. INTRODUCTION

The phenomena of combustion in a rocket motor belong essentially to the class of high temperature, fast reactions. A detailed study of the kinetics of such reactions in a rocket motor would involve a long period of time and a large expenditure of funds. One simplified approach to this study of combustion involves an investigation of possible relationships among flame speed, slow oxidation, and actual operating rocket motor characteristics.

Laboratory studies of relative apparent flame speeds and independent investigations of the relative slow oxidation rates as measured by the rate of evolution of CO<sub>2</sub> from several fuel-oxygen systems have been carried out at Reaction Motors, Inc. (Ref. 1). Under these same studies, propellant performance as a function of the chamber volume (or length) and of the flow rate in an 11-pound-thrust-chamber motor has been studied for similar fuel-liquid oxygen systems. The fuels studied were ethane, ethanol, ethylamine, and acetaldehyde. Two empirical linear relationships have been postulated as a result of these preliminary studies. These are

$$V_a = \frac{-2.09}{m} + 4.58$$

$$\log \frac{1}{m} = (0.200 \times 10^{-4}) \frac{V}{W^3} - 1.472$$

where  $V_a$  = maximum apparent flame speed

$m$  = slope of the % CO<sub>2</sub> evolved vs log contact time from the slow oxidation studies

$V$  = combustion chamber volume of the 11-lb-thrust motor

$W$  = total flow rate of propellants to the combustion chamber of the motor.

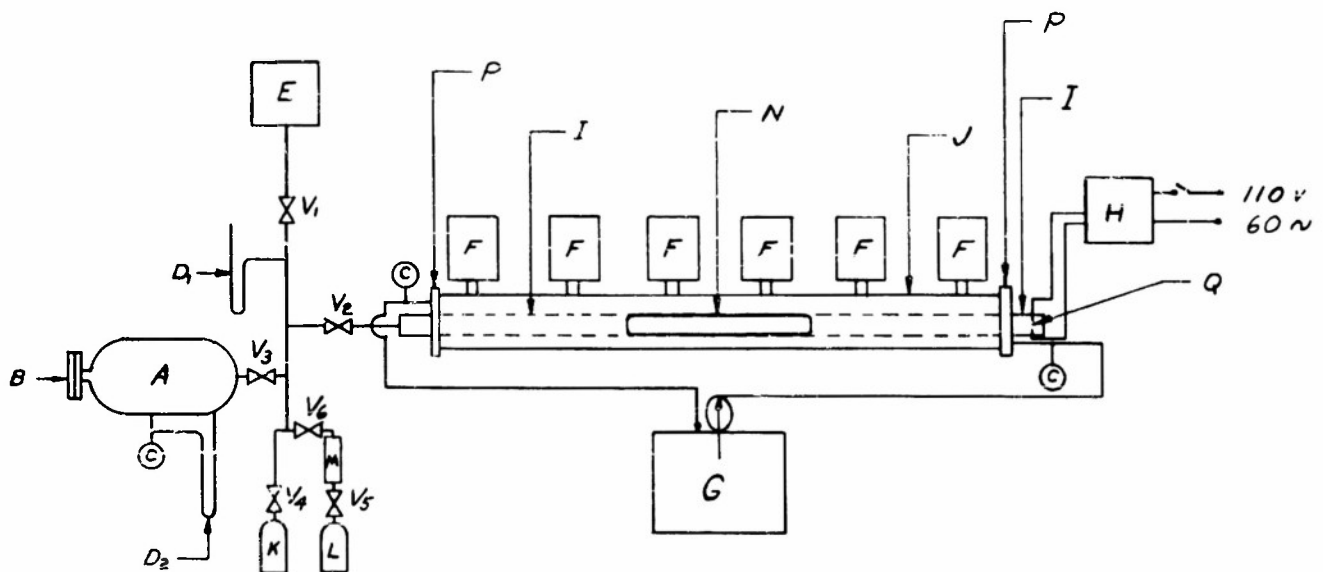
In order to determine the validity of the above relationships, under the present contract additional fuel-oxidizer systems have been studied with the same type of equipment and methods as were used in the previous investigation. The fuels chosen were ethylene oxide, cyclopropane, ethylene, and ammonia.

3. FLAME SPEED MEASUREMENTS3.1 Apparatus

The horizontal tube method was employed to obtain the flame speed data. A schematic drawing of the flame speed apparatus is given in Fig. 1. This apparatus consists of three units, (a) the mixing chamber, (b) the flame tube and temperature control, and (c) the electronic recording system.

a. Mixing Chamber. The ellipsoidal stainless steel mixing tank (A) has a capacity of approximately 540 cu in. A circular rupture disc (B) is attached on one end of the mixing tank; in the event that too high a pressure is reached the disc will rupture. This disc is made of sheet aluminum 3 in. in diameter and 0.006 in. in thickness and is flanged by two stainless steel circular plates. The tank is resistance heated by a nichrome wire coil.

b. Flame Tube and Temperature Control. The flame tube (I) is a 4-ft length of 1-1/8 in. I. D. pyrex glass tubing into which two tungsten electrodes (Q) are diametrically sealed. These electrodes are connected to a 10,000 volt ignition transformer (H). The flame tube is



A. MIXING TANK  
B. RUPTURE DISC  
C. THERMOCOUPLE  
D. MERCURY MANOMETER

E. VACUUM PUMP  
F. PHOTOTUBE  
G. HEATING BATH &  
CIRCULATING PUMP  
H. 10000 V IGNITION  
TRANSFORMER

I. FLAME TUBE  
J. WATER JACKET  
K. FUEL SUPPLY  
L. COMPRESSED AIR

M.  $\text{CaCl}_2$  DRYING TUBE  
N. TRANSPARENT "WINDOW"  
OF FLAME TUBE  
O. VALVE  
Q. TUNGSTEN ELECTRODES  
P. FLANGES, STAINLESS STEEL  
WITH RUBBER GASKET

FIGURE 1

FLAME SPEED APPARATUS - SCHEMATIC

painted black on the outside except for 1 in. bands at intervals of 7-1/2 in. and the area corresponding to (N). The flame tube is enclosed in a 3 in. I. D. glass tube which serves as a water jacket. This outer tube is made water tight by a pair of stainless steel plate flanges with rubber gaskets (P) and is insulated by MgO pipe lagging except for the ports opposite the bands in the flame tube. The "window" (N), through which motion pictures of the flame may be taken as it travels along the length of the tube, is cut through the MgO lagging. The flame tube is maintained at a temperature of  $81.0 \pm 0.3^\circ\text{C}$  by means of the constant temperature bath and circulating system (G). The temperatures in the mixing tank (A) and of the water in the jacket (J) are measured by copper-constantan thermocouples (C).

c. Electronic Recording System. The electronic recording system consists of six RCA phototubes, type 1P29, a DuMont oscilloscope, type 304H; a Hewlett - Packard low frequency audio oscillator, type 202A, with an audio transformer; and a Fairchild Oscillo-Record camera, model F-246. For the ammonia-air system the 1P29 phototubes were replaced by phototubes 868 since the latter are more sensitive to the wave lengths emitted by the resulting pale orange yellow flame. The phototubes (F) are mounted separately in 3 x 4 x 5 in. metal boxes fitted with 1 in. I. D. sight tubes. The sight tubes fit into the ports in the MgO lagging and are directly opposite the bands of the flame tube. The phototubes are wired in parallel (appropriately shielded) and connected to the input side of an oscilloscope. The electronic and photocell wiring diagram is schematically represented in Fig. 2. A

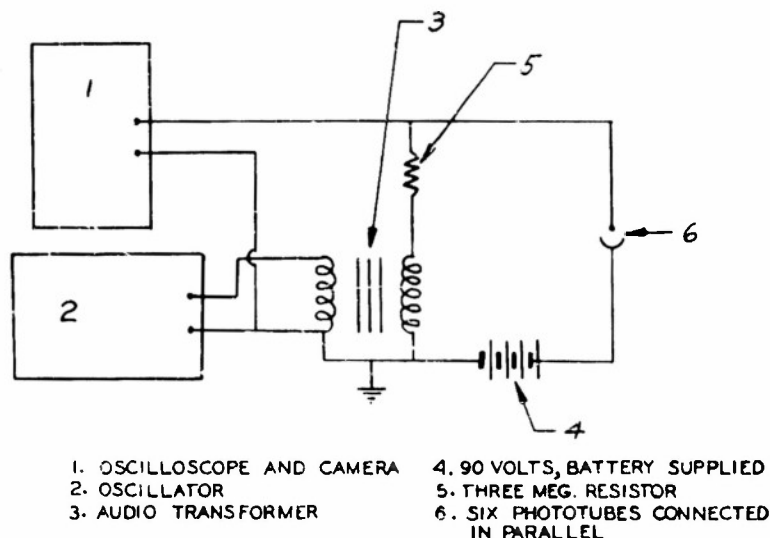


FIGURE 2  
 ELECTRONIC AND PHOTOCCELL WIRING DIAGRAM - SCHEMATIC

connection from the Hewlett - Packard oscillator is made to the input side of the oscilloscope thus introducing a low amplitude, one kilocycle standard time trace which is photographed along with the timing signals by the Fairchild Oscillo-Record camera.

### 3.2 Operational Procedure

The flame tube (I) and the mixing tank (A) are first raised to the desired temperature (81°C). The mixing tank and flame tube (with a rubber stopper at the ignition end) are then evacuated. With valves  $V_1$ ,  $V_2$ , and  $V_6$  closed, the fuel from K is introduced into the tank and its pressure measured manometrically by  $D_2$ . With  $V_3$  and  $V_4$  closed, the supply lines are again evacuated and then  $V_1$  is closed. The air from tank L, dried by passing through a  $\text{CaCl}_2$  tube (M), is introduced into the mixing tank and the total pressure recorded by manometer  $D_2$ . From the two measured pressures, the air-to-fuel ratio is easily determined. The total pressure must be sufficiently above one atmosphere so that three runs for each air-to-fuel ratio may be made from a single tank filling. The evacuated flame tube is then filled with the heated combustible mixture until the pressure in the tube is equal to the atmospheric pressure as measured by manometer  $D_1$ . At this point, valve  $V_2$  is closed and the rubber stopper is replaced by a porous plug consisting of a coiled 2-1/2 in. wide strip of 0.005 in. thick shim brass. This plug serves as a damping mechanism for the resonating effect developed by the moving flame. The Oscillo-Record camera is now put into operation and the mixture ignited. The above process is repeated for four to five different air-to-fuel ratios.

A typical record of an ethane-air flame as it moved past the fourth, fifth, and sixth photocells is depicted in Fig. 3. The oscillogram is projected on a graphical screen and the distances (inches) between maxima (pips) are determined. The projected oscillogram consists of a large number of closely spaced sine waves wherein each complete wave represents a time trace of one millisecond. Although they are



Figure 3  
Recorded Oscillogram of an Ethane-Air Flame

not visible in the recorded oscillogram of Fig. 3, these waves may readily be seen on an enlarged projection. The computed mean time interval between pips is directly related to the actual time interval necessary to traverse 7-1/2 in. (the distance between phototubes). The mean apparent flame speed over the length of the tube corresponding to three runs at a definite air to fuel ratio may then be easily computed.

### 3.3 Analysis of Data

Apparent flame velocities of the ethylene, cyclopropane, and ethylene oxide systems with air as oxidizer have been measured at various mixture ratios over the entire range of flammability limits. The average apparent flame velocities over the entire flame tube length are listed in Table 1. Plots of these apparent flame velocities,  $V_a$  (cm/sec) vs composition (in volume percent) are given in Fig. 4.

No data for ammonia are reported because of the difficulty experienced in igniting and propagating the resulting flame from ammonia-air mixtures over the flammability limits of 16 to 27% (Ref. 2). This marked inertness of ammonia in non-catalytic combustion processes has been reported by other workers. Stephens and Pease (Ref. 3) showed that a small jet of ammonia in air will not support a stable flame. Furthermore, according to these workers, a stoichiometric ammonia-air mixture at room temperature and pressure is not ignited by a spark from a small induction coil. White (Ref. 4), however, was able to initiate upward (but not downward) propagation in ammonia-air mixtures at atmospheric pressure in a 5-cm glass tube by exploding 1 to 2 mg of guncotton yarn in the mixture. No mention was made by this author of experiments in a horizontal tube.

### 3.4 Discussion of Data

The data presented in Table 1 are the results of a study of apparent flame velocities of ethylene, cyclopropane, and ethylene oxide. A graph of apparent flame velocity vs volume percent fuel in mixture is depicted in Fig. 4 from which the maximum apparent flame velocities 169 cm/sec for ethylene, 109 cm/sec for cyclopropane and 266 cm/sec for ethylene oxide were taken.

It should be noted that the maximum flame velocities reported are not fundamental flame velocities and further are measured at an initial mixing temperature of 81°C. Flame velocity data are more commonly given at 25°C and in the form of fundamental flame velocity. Hence, inasmuch as fundamental flame speeds were not determined, no attempt is made to compare the flame speed data of this report with those of other workers.

TABLE I  
APPARENT FLAME SPEED DATA

<u>FUEL</u>	<u>Volume Percent Fuel in Mixture</u>	<u>Apparent Flame Speed (cm/sec.)</u>
Ethylene	9.29	163
	9.37	158
	9.51	170
	9.77	169
	11.00	128
Cyclopropane	5.10	96
	6.01	111
	6.23	106
	6.30	108
	6.79	102
Ethylene Oxide	6.50	187
	7.62	132
	8.21	197
	9.21	204
	9.49	293
	9.50	249
	9.60	311
	10.69	239
	11.17	262
	11.66	309
	12.93	149
14.58	96	

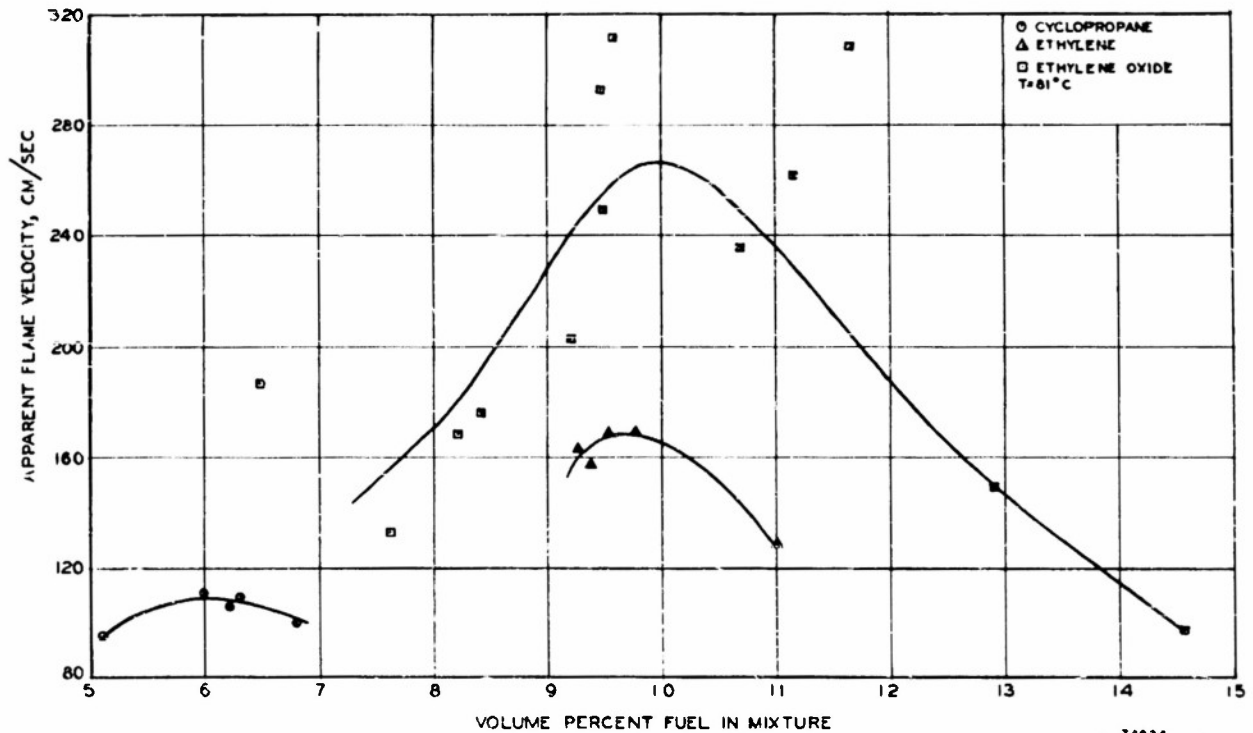


FIGURE 4  
APPARENT FLAME SPEED VS PERCENT FUEL IN MIXTURE

74024  
(REPORT DWG)

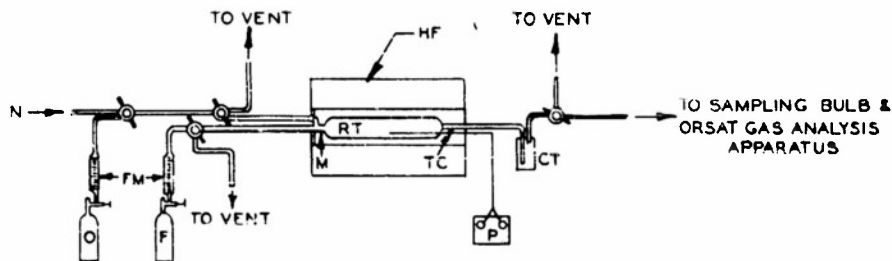
#### 4. SLOW OXIDATION STUDIES

In general, two types of systems may be used to carry out slow oxidation studies. These are (a) a closed or static system and (b) an open or flow system. Inasmuch as the combustion process in a rocket motor is simulated by the flow method, the latter has been used in these and previous (Ref. 1) slow oxidation studies. In the flow system, mixtures of reactants of known initial composition flow, at approximately atmospheric pressure, through a region of reaction of known volume at a known rate. Analysis of the mixture is made after passage through the reaction space.

##### 4.1 Apparatus

A schematic diagram of the slow oxidation flow apparatus is depicted in Fig. 5. Fuel (F) and oxygen (O), each of 99.5% purity obtained in cylinders from the vendor, were used in all experiments. The rate of flow of reactants was controlled by means of low flow rate (FM) Fischer & Porter Tri-Flat flowmeters. Calibration curves for these meters were constructed from the densities and viscosities of the various fuels and oxygen by a method described in the Fischer-Porter Handbook accompanying these meters. These curves were checked experimentally by water displacement in the case of oxygen and by a simple "freezing-out" method in the case of the fuels. The agreement between the experimental and theoretical curves was satisfactory.

The cylindrical reaction tube (RT) was of pyrex, 32 mm in diameter



F = FUEL SUPPLY  
 O = OXYGEN SUPPLY  
 FM = FISCHER-PORTER TRI-FLAT TUBE  
 FLOWMETER  
 N = NITROGEN INLET

RT = REACTOR TUBE  
 HF = HOSKINS ELECTRIC FURNACE  
 TC = THERMOCOUPLE  
 CT = COLDTRAP

(48714  
 REPORT DWC)

FIGURE 5  
 SLOW OXIDATION FLOW APPARATUS—SCHEMATIC

and 26 cm long, with a reaction volume of 171 cc. A short length (approximately 1 cm) of tubing (M) joined to the reaction tube served as a mixing region. The reaction tube was set in a tubular Hoskins electric furnace (HF), type FD 303A, the temperature of which was controlled by a 0 to 135 volt Variac (not shown) and measured with a calibrated Chromel-Alumel thermocouple (TC) and potentiometer (P). The exhaust products and unreacted reactants were passed through a trichloroethylene-dry ice trap (CT) and then into a sampling bulb attached to a Fisher precision gas analysis apparatus of the Orsat type. The operation of the latter is adequately described in a manual published by the Fisher Scientific Co., Pittsburgh, Penna.

#### 4.2 Operational Procedure

In operation, the furnace is brought to the desired temperature of about 350°C. The oxygen and fuel flow rates are then set at predetermined values corresponding to the O/F (b. w.) ratio at which the experimental maximum C\* occurs in the 11-pound thrust motor for the particular system under consideration. The reactants are vented during this operation. After the flow rates are set and the furnace temperature controlled at 350 ± 3°C, the reactants are allowed to pass through the reaction tube. The resulting mixture is then passed through the cold trap (CT) which is maintained at -71 ± 1°C. The reaction is allowed to proceed for at least an hour during which the non-condensable gases are vented. After an "aging" time of 1 to 2 hours, the non-condensable gases are appropriately sampled without disturbing the flow rates and finally analyzed for CO<sub>2</sub>, illuminants (if any), O<sub>2</sub>, and CO. Four to six runs are made at each contact time, i. e. the time of residence in the reaction zone. The contact time (sec) is equal to the total volume (cc) of the reaction zone divided by the total flow rate (cc/sec) at the entrance to the reaction zone. Each fuel-oxygen system is measured at four different contact times at a definite O/F (b. w.) ratio. For each change of fuel, the reaction tube is cleaned with chromic acid, copiously rinsed with distilled water, and dried before reuse.

#### 4.3 Analysis of Data

Slow oxidation studies on the systems ethylene oxide, cyclopropane, and ethylene with oxygen as the oxidizer have been carried out at 350 ± 3°C. The latter represents the temperature at approximately the center of the reaction tube. The resultant data with their respective standard deviations are presented in Table 2. The percentages in the table represent the mean of the analyses of the exhaust gases which have passed through the cold trap (-71°C). Four to six runs were made at each contact time with a single analysis being performed for each run. A criterion for the rejection of individual observations has been used in

TABLE 2  
SLOW OXIDATION DATA

Fuel	Contact Time (sec)	% CO <sub>2</sub>	% Fuel	% O <sub>2</sub>	% CO	% Residue
Ethylene Oxide P/O = 1.64 ± 0.16	10	5.7 ± 0.5	—	87.8 ± 1.6	0.4 ± 0.2	4.2 ± 0.9
	18	3.6 ± 0.7	—	91.5 ± 1.3	0.2 ± 0.0	4.6 ± 1.4
	59	3.4 ± 0.6	—	82.3 ± 2.0	2.5 ± 0.7	12.2 ± 2.0
	125	3.1 ± 0.3	—	88.5 ± 2.8	0.4 ± 0.2	8.1 ± 2.4
Cyclopropane P/O = 2.05 ± 0.21	63	~0.0*	—	85.4 ± 0.9	10.7 ± 1.0	3.9 ± 1.3
	148	~0.0*	—	84.2 ± 2.1	9.6 ± 1.0	6.0 ± 1.2
	190	~0.0*	—	85.6 ± 1.1	9.5 ± 1.5	4.5 ± 0.4
	333	~0.0*	—	86.5 ± 1.9	10.1 ± 1.2	3.2 ± 0.8
Ethylene P/O = 2.22 ± 0.22	101	0.2 ± 0.1	32.1 ± 0.8	62.8 ± 1.7	0.1 ± 0.1	4.4 ± 0.8
	174	0.7 ± 0.2	28.4 ± 4.2	57.8 ± 3.7	2.4 ± 1.4	9.7 ± 6.5
	258	0.9 ± 0.4	22.1 ± 4.8	56.2 ± 2.1	0.2 ± 0.2	11.8 ± 6.3
	418	1.4 ± 0.6	23.5 ± 3.7	54.6 ± 2.8	6.0 ± 3.7	5.6 ± 0.8

\* The amount of CO<sub>2</sub> evolved was so small that it could not be determined with the apparatus.

computing the results. This involved computing the mean and the standard deviation,  $S$ , omitting the doubtful observation. The deviation,  $d$ , of the doubtful observation from the mean was also computed. If  $d \geq 4S$ , then the doubtful observation was rejected.

It can easily be shown that the contact time is inversely proportional to the volume rate of flow of fuel or oxygen assuming a total constant pressure. The latter was tacitly assumed to be one atmosphere. Thus, the contact times in Table 2 are within  $\pm 7\%$  which is the uncertainty in the individual flowrates. Furthermore, in computing the contact time, it was assumed that the total volume rate of flow of reactants entering the reaction tube is equal to the total volume rate of flow of products and unreacted reactants as the reaction progresses in the reaction zone. It was necessary to make this assumption because of the complexity of the reactions under study.

In the slow oxidation studies described in Ref. 1, the percent of CO<sub>2</sub> evolved was plotted vs the logarithm of the contact time (Fig. 19) for the systems ethane, ethanol, acetaldehyde, and ethylamine with oxygen at 350°C. These data together with the data from Table 2 of this report are plotted in Fig. 6.

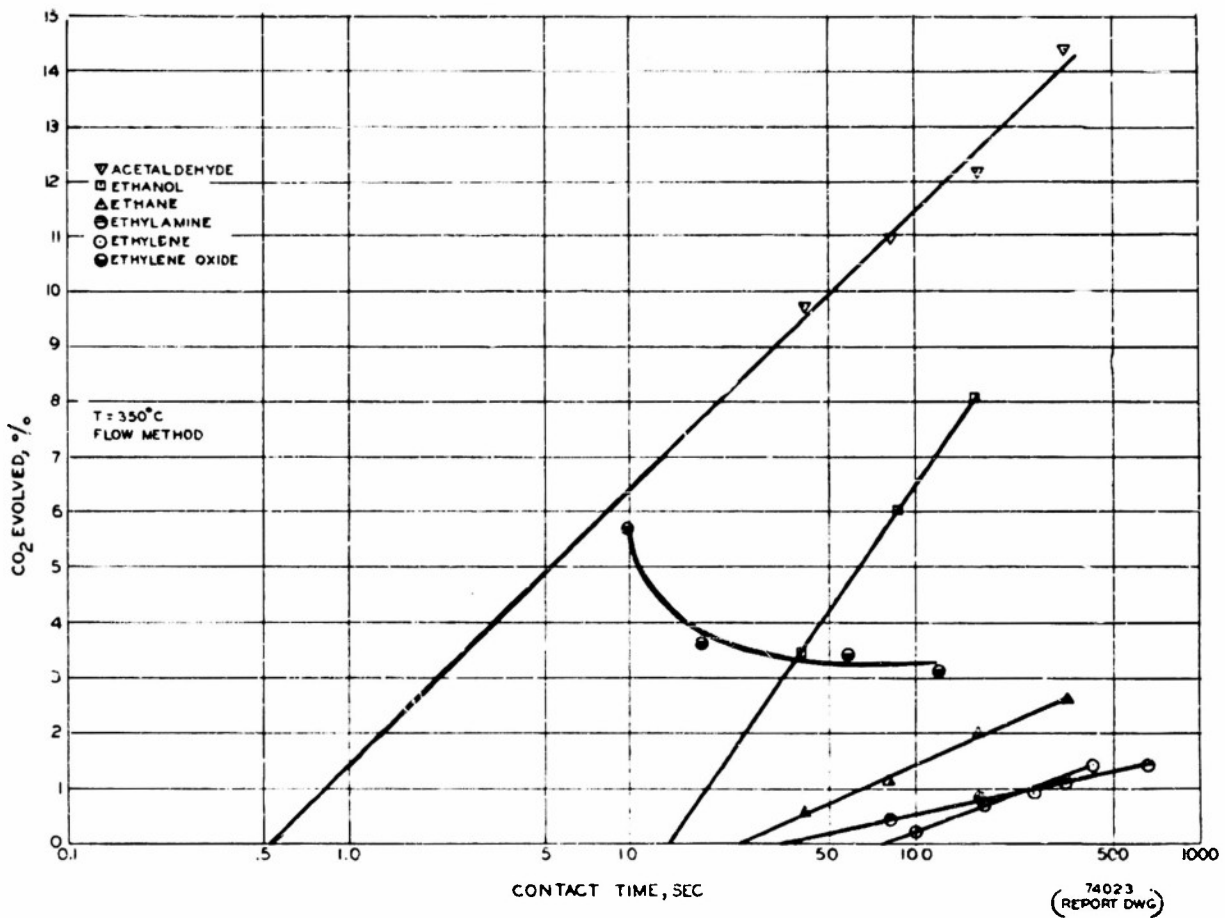


FIGURE 6  
PERCENT CO<sub>2</sub> EVOLVED VS CONTACT TIME

#### 4.4 Discussion of Data

A cursory examination of the slow oxidation data in Table 2 reveals the fact that cyclopropane does not yield a measurable amount of CO<sub>2</sub> under the conditions of the reaction. In the plot of percent CO<sub>2</sub> versus the logarithm of the contact time, Fig. 6, it is readily seen that of the two remaining fuels studied under this contract, only ethylene yields a straight line. The percent CO<sub>2</sub> evolved from the ethylene oxide-oxygen system decreases with increasing contact time. The ethylene curve may be represented by the general equation

where

$$\% \text{CO}_2 = m \log t + b$$

m = slope of the line  
t = contact time in seconds  
b = constant = hypothetical % CO<sub>2</sub> at t=1 sec.

Using the method of least squares the constants m and b turn out to be 1.908 and -3.626 respectively. Thus, the ethylene curve is specifically represented by

$$\% \text{CO}_2 = 1.908 \log t - 3.626$$

The induction period, i. e., the contact time required for the first formation of carbon dioxide from the ethylene-oxygen system at 350°C is approximately 79 sec.

Slow oxidation studies on the ammonia-oxygen system were not attempted inasmuch as the substantiation of the postulated relationships in Ref. 1 involved the determination of the quantity of CO<sub>2</sub> evolved from various fuel-oxygen systems at 350°C as a function of the logarithm of the contact time.

In scrutinizing the data of Table 2 it should be kept in mind that the percent CO<sub>2</sub> includes any possible acidic gases which may have passed through the cold trap at -71°C.

## 5. ROCKET MOTOR INVESTIGATION

In Ref. 1, rocket motor characteristic data i. e. , total flow rate and the minimum chamber volume for optimum performance have been obtained using a water-cooled 11-pound -thrust motor. With some minor modifications, this motor has been reassembled for use in this phase of the current program.

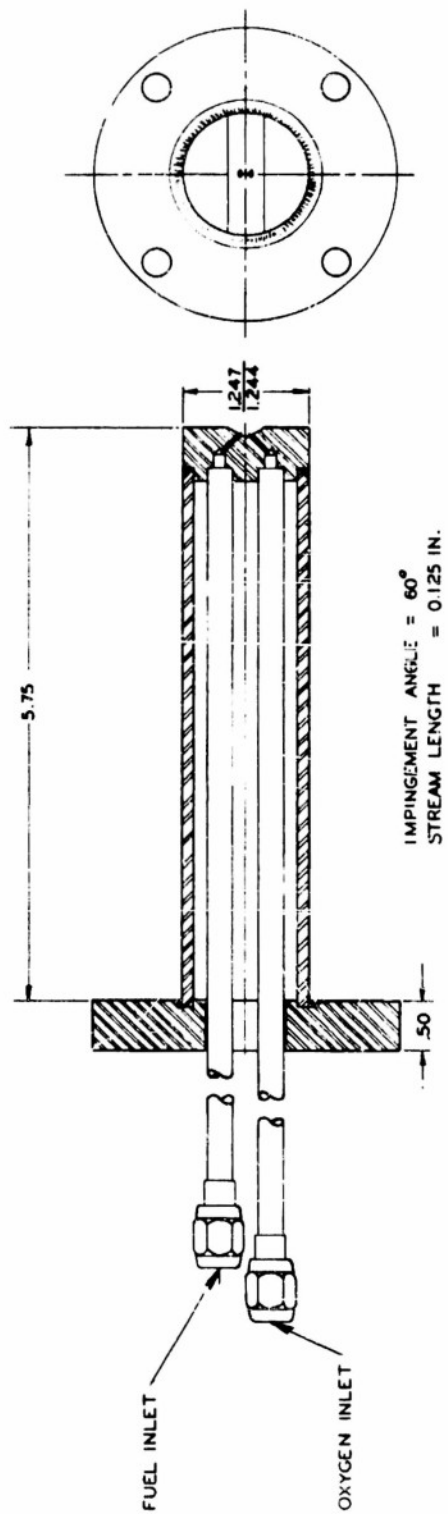
### 5.1 Apparatus

The combustion chamber of the water-cooled 11-pound-thrust motor is cylindrical in shape, hence, minimum chamber volume becomes synonymous with minimum chamber length. A stainless steel, two stream one-on-one impinging type injector was fabricated in such a manner as to fit into the combustion chamber as a piston fits into a cylinder. The barrel of the injector is 5-3/4 in. in length. Figure 7 shows a diagram of this injector. Two cylindrical copper motors which would accommodate the injector were fabricated. Figure 8 shows an 11-pound-thrust chamber with the variable position injector in place. One of these motors has an over-all length of 8.5 in. and the other an over-all length of 14.5 in. The chamber length can be varied in increments of one inch by placing one inch separators between the injector and chamber flanges. Chamber lengths of one to six inches are obtained by using the 8.5 in. motor while chamber lengths of seven to twelve inches are available with the 14.5 in. motor. Hence, the chamber volume may be varied by a factor of one to twelve.

A small portable test stand, on which the motor is mounted, has been assembled together with the accessory equipment necessary for transferring the propellants to the combustion chamber. Figure 9 is a schematic drawing of the components of the portable test stand. These components consist of the oxidizer system and the fuel system.

The oxidizer system consists of a stainless steel tank, approximately 1-3/4 gal in capacity submerged in a Dewar flask containing liquid nitrogen. Helium (B) is used to pressurize the liquid oxygen by means of a Marotta MV40 pressurizing and vent valve (C). The helium is passed through the heating coil (D) and cold trap (E) and then into the oxygen propellant tank (A). The purpose of the heating coil (D) is to vaporize any liquid oxygen and/or helium prior to venting the tank through the valve (C), thus eliminating the possibility of freezing this valve in an open position. The cold trap (E) removes any condensable contaminants present in the helium.

In operation, the liquid oxygen proceeds through a metering orifice (F), then through a motorized metering valve (G), and finally through a prop



46533

FIGURE 7

VARIABLE POSITIONING INJECTOR FOR  
ELEVEN POUND THRUST CHAMBER

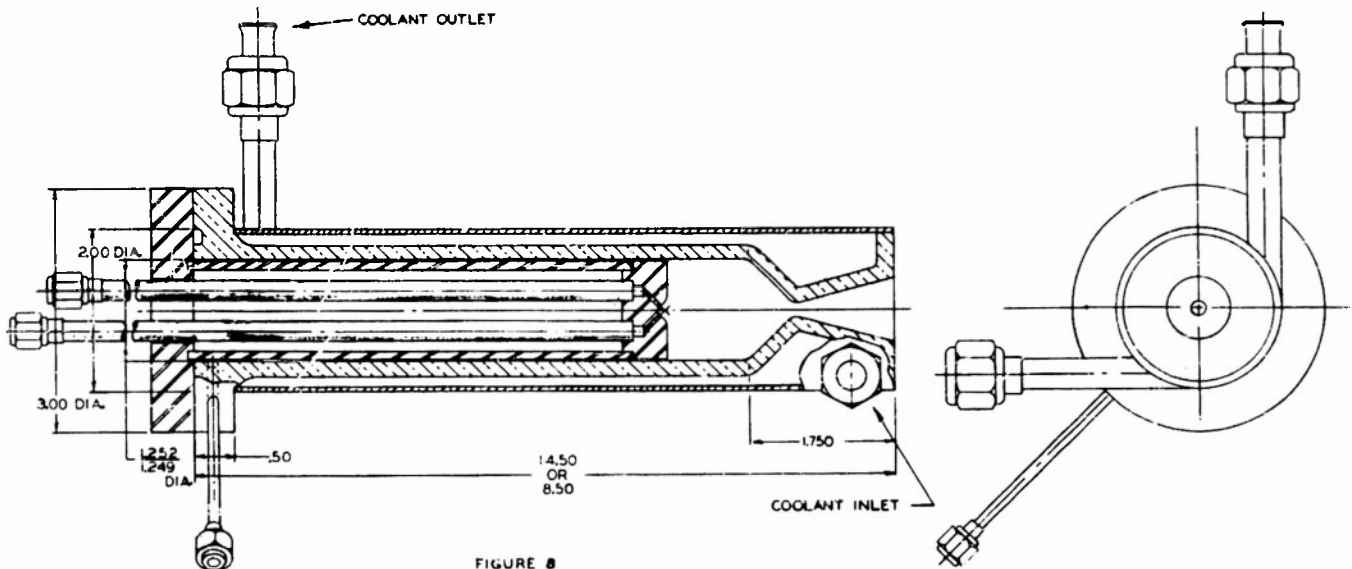
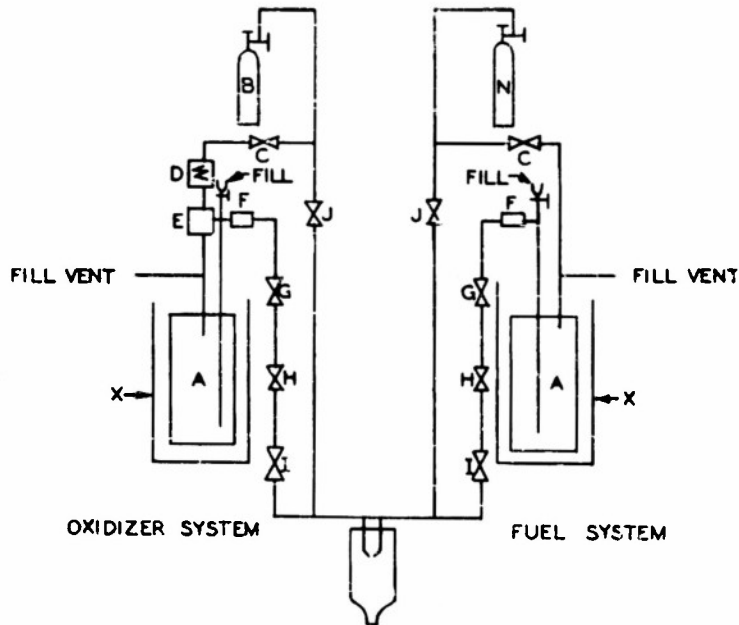


FIGURE 8  
ELEVEN POUND THRUST CHAMBER WITH A  
VARIABLE POSITION INJECTOR



- |  |  |
|--|--|
| A. PROPELLANT TANK                         | F. METERING ORIFICE CONNECTED TO THE BARTON FLOWMETERS |
| B. SOURCE OF HELIUM                        | G. MOTORIZED METERING VALVE                            |
| C. MAROTTA MV 40 PRESSURIZING & VENT VALVE | H. PROP VALVE  |
| D. HEATING COIL                            | I. CHECK VALVE   |
| E. COLD TRAP                               | J. BLOWDOWN VALVE                                      |
| N. SOURCE OF NITROGEN                      |  |
| X. D&WAR FLASK                             |  |

FIGURE 9  
THE PORTABLE TEST STAND - SCHEMATIC

46531

valve (H). The latter enables the operator to commence and terminate a run without the necessity of opening and/or closing the metering valve (G) which operates too slowly for fast shutdowns. The prop valve also initially enables one to set the oxygen and fuel flows at any specific O/F ratio. A check valve (I) is used to sustain a flow in a positive direction, i. e., from the liquid oxygen tank (A) to the combustion chamber. Valve (I) also prevents the possibility of any combustible mixture seeping back into the oxygen tank (A). The blowdown valve (J) is used to purge the system after each run.

As Fig. 9 shows, the fuel system is practically identical with the oxidizer system with nitrogen (N) being used as the fuel pressurizing gas. All valves and vents for both the fuel and oxidizer systems are operated by remote control from an instrument panel. Figures 10 and 11 are photographs of the test stand and instrument panel, respectively.

## 5.2 Operational Procedure

The oxygen and fuel Barton Differential pressure flowmeters are calibrated for each fuel to be run. The motor is set at a definite chamber

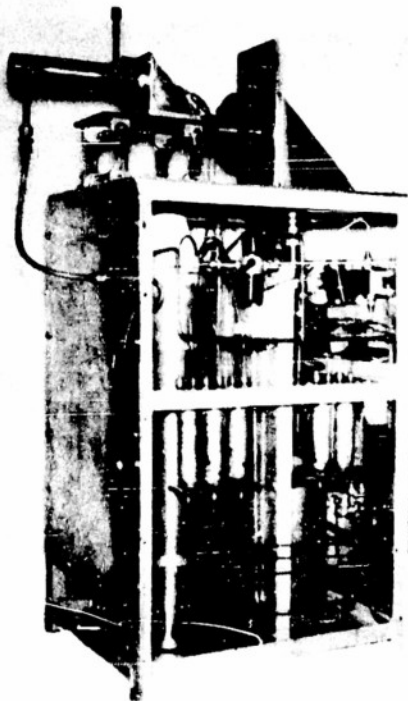


Figure 10

11-Pound-Thrust Motor Unit  
and Stand

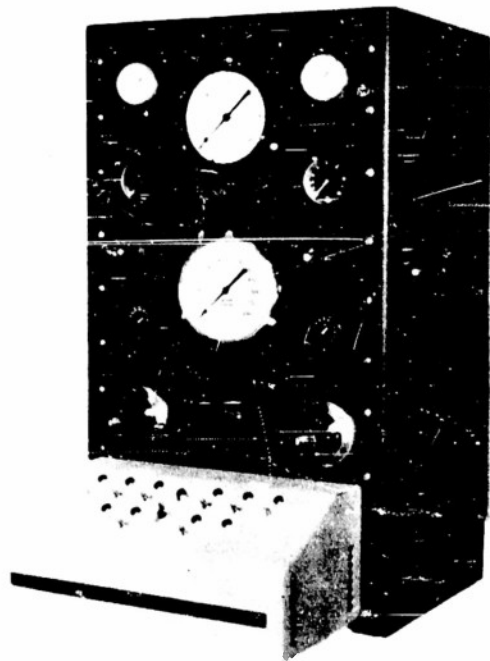


Figure 11

Instrument Control Panel for  
11-Pound-Thrust Unit

length. The oxygen tank is cooled in a Dewar flask containing liquid nitrogen and then charged with liquid oxygen. Similarly, the fuel tank is cooled in a Dewar flask containing alcohol and/or petroleum ether in liquid nitrogen and charged under the fuel pressure directly from the vendor tanks. The desired pressures are obtained in the propellant tanks, the operation of all electrically controlled valves checked, an electrically ignited solid propellant squib inserted into the nozzle of the motor, and the motor fired. The fuel and oxygen flow-rates are successively set at six to seven predetermined points in order to obtain the desired O/F ratios and a constant total mass flow rate. The gage chamber pressure is recorded at each point and converted to the pressure in psia. The chamber length is changed and the process repeated.

### 5.3 Analysis of Data

The pertinent rocket motor characteristics which have been used in a possible correlation suggested in Ref. 1 are the total flow rate and the minimum chamber volume for optimum performance using the characteristic velocity  $C^*$  as the performance parameter. This quantity is defined by the equation

$$C^* = \frac{P_c A_t g}{W} \quad (1)$$

where  $P_c$  = chamber pressure in psia

$A_t$  = cross sectional area of the throat in sq in.

$g$  = gravitational constant = 32 ft/sec<sup>2</sup>

$W$  = total mass flow rate in lb/sec

The throat area,  $A_t$ , is measured after each chamber length run. The characteristic velocity  $C^*$  is computed from the experimentally determined  $P_c$  and  $A_t$  values with the total flow rate,  $W$ , being 0.050 lb/sec for all systems except ethylene-lox which was measured at a total flow rate of 0.061 lb/sec. The results are recorded in Tables 3 through 6 and the computed characteristic velocities are plotted vs the O/F mixture ratio by weight for each fuel-lox system at various chamber lengths in Figs. 12 through 15.

### 5.4 Discussion of Data

The conditions during the accumulation of the data reported herein were similar to those presented in Ref. 1 so that the data may be compared with those already reported. In these operations only chamber pressure and flow rate measurements were made. No attempt was made to record thrust performance, since this parameter was not investigated previously. Since this study was not concerned with a design investigation but rather with the

TABLE 3

EXPERIMENTAL C\* AT VARIOUS CHAMBER LENGTHS  
ETHYLENE - LIQUID OXYGEN (1)

Chamber Length, 3 in. Throat Area, $A_t$ , 0.0366 sq in.			Chamber Length, 4 in. Throat Area, $A_t$ , 0.0366 sq in.		
O/F	$P_c$ psia	C*(2) ft/sec	O/F	$P_c$ psia	C* ft/sec
1.82	300	5760	1.85	330	6340
2.05	305	5860	2.05	335	6430
2.21	305	5860	2.27	337	6510
2.49	310	5950	2.46	337	6470
2.62	310	5950	2.69	335	6430

TABLE 4

EXPERIMENTAL C\* AT VARIOUS CHAMBER LENGTHS  
CYCLOPROPANE - LIQUID OXYGEN (1)

Chamber Length, 4 in. Throat Area, $A_t$ , 0.0284 sq in.			Chamber Length, 5 in. Throat Area, $A_t$ , 0.0336 sq in.		
O/F	$P_c$ psia	C* ft/sec	O/F	$P_c$ psia	C* ft/sec
1.25	267	4850	1.80	250	5380
1.50	285	5180	1.92	255	5460
1.51	290	5270	1.99	255	5480
1.55	280	5090	2.05	257	5530
1.71	285	5180	2.18	255	5480
1.91	285	5180	2.38	248	5330
2.05	275	5000			
2.10	275	5000			

Chamber Length, 5 in. Throat Area, $A_t$ , 0.0366 sq in.			Chamber Length, 6 in. Throat Area, $A_t$ , 0.0366 sq in.		
O/F	$P_c$ psia	C* ft/sec	O/F	$P_c$ psia	C* ft/sec
1.64	315	6050	1.20	305	5860
1.83	322	6180	1.73	307	5890
2.05	320	6140	1.82	308	5910
2.27	335	6430	2.05	314	6030
2.48	330	6340	2.46	309	5930
2.69	327	6280			

Chamber Length, 6 in. Throat Area, $A_t$ , 0.0336 sq in.			Chamber Length, 7 in. Throat Area, $A_t$ , 0.0306 sq in.		
O/F	$P_c$ psia	C* ft/sec	O/F	$P_c$ psia	C* ft/sec
1.56	240	5160	1.77	280	5480
1.80	255	5480	1.77	275	5390
1.94	255	5480	1.91	279	5460
2.00	245	5270	1.92	278	5440
2.10	247	5310	1.98	277	5420
2.18	250	5380	2.00	280	5480
2.40	251	5400	2.09	275	5390
			2.21	275	5390
			2.21	270	5290

(1) A total flow rate of 0.061 lb/sec was maintained.

(2) Although the instrumentation does not warrant four significant figures, data in this and subsequent tables for C\* are reported as such because of the established convention of presenting performance data throughout the rocket industry.

(1) A total flow rate of 0.050 lb/sec was maintained.

determination of relative performance efficiency under similar design conditions, the injector used was the same for every fuel-liquid oxygen system.

Some difficulty with injector burnouts was encountered during the ethylene operations. However, by increasing the total flow rate, the frequency of injector burnouts was diminished.

TABLE 5  
EXPERIMENTAL C\* AT VARIOUS CHAMBER LENGTHS  
AMMONIA - LIQUID OXYGEN (1)

Chamber Length, 5 in. Throat Area, A <sub>t</sub> , 0.0305 sq in.		
<u>O/F</u>	<u>P<sub>c</sub> psia</u>	<u>C* ft/sec</u>
1.00	250	4880
1.25	260	5080
1.35	258	5040
1.40	258	5040
1.50	255	4920
1.69 <sup>m</sup>	250	4880
1.71	260	5080

Chamber Length, 6 in. Throat Area, A <sub>t</sub> , 0.0305 sq in.			Chamber Length, 7 in. Throat Area, A <sub>t</sub> , 0.0281 sq in.		
<u>O/F</u>	<u>P<sub>c</sub> psia</u>	<u>C* ft/sec</u>	<u>O/F</u>	<u>P<sub>c</sub> psia</u>	<u>C* ft/sec</u>
0.75	240	4680	0.75	265	4770
1.00	260	5080	1.00	280	5040
1.27	269	5250	1.26	290	5220
1.40	272	5310	1.40	278	5000
1.50	270	5270	1.46	277	4980

Chamber Length, 8 in. Throat Area, A <sub>t</sub> , 0.0286 sq in.			Chamber Length, 9 in. Throat Area, A <sub>t</sub> , 0.0298 sq in.		
<u>O/F</u>	<u>P<sub>c</sub> psia</u>	<u>C* ft/sec</u>	<u>O/F</u>	<u>P<sub>c</sub> psia</u>	<u>C* ft/sec</u>
0.98	270	4940	1.24	265	5050
1.25	277	5070	1.34	270	5150
1.40	280	5130	1.41	272	5190
1.50	283	5180	1.50	270	5150
1.70	280	5130			
1.80	280	5130			

(1) A total flow rate of 0.050 lb/sec was maintained.

Little difficulty was encountered during the operation of the other fuel combinations, however, the cyclopropane-liquid oxygen combination produced low frequency vibration, which could be described as "chugging".

TABLE 6  
EXPERIMENTAL C\* AT VARIOUS CHAMBER LENGTHS  
ETHYLENE OXIDE-LIQUID OXYGEN (1)

Chamber Length, 4 in.  
Throat Area,  $A_t$ , 0.0284 sq in.

<u>O/F</u>	<u>P<sub>c</sub> psia</u>	<u>C* ft/sec</u>
1.00	280	5090
1.06	282	5130
1.28	285	5180
1.43	287	5220
1.54	290	5270
1.79	280	5090
2.04	260	4730

Chamber Length, 5 in.  
Throat Area,  $A_t$ , 0.0278 sq in.

<u>O/F</u>	<u>P<sub>c</sub> psia</u>	<u>C* ft/sec</u>
0.99	293	5210
1.22	301	5360
1.30	305	5430
1.45	300	5340
1.52	297	5280
1.69	295	5250
1.78	287	5110
2.00	300	5340
2.04	260	4630

Chamber Length, 6 in.  
Throat Area,  $A_t$ , 0.0282 sq in.

<u>O/F</u>	<u>P<sub>c</sub> psia</u>	<u>C* ft/sec</u>
1.01	288	5200
1.08	287	5180
1.38	290	5230
1.39	290	5230
1.59	295	5320
1.70	290	5230
1.79	270	4870
1.83	282	5090

Chamber Length, 7 in.  
Throat Area,  $A_t$ , 0.0272 sq in.

<u>O/F</u>	<u>P<sub>c</sub> psia</u>	<u>C* ft/sec</u>
1.00	285	4960
1.25	292	5080
1.52	305	5310
1.60	317	5520
1.77	315	5480
1.78	313	5450
1.87	311	5410
2.00	315	5490

Chamber Length, 8 in.  
Throat Area,  $A_t$ , 0.0272 sq in.

<u>O/F</u>	<u>P<sub>c</sub> psia</u>	<u>C* ft/sec</u>
1.02	295	5140
1.02	298	5190
1.27	295	5140
1.28	305	5310
1.50	308	5360
1.52	307	5340
1.77	311	5410
1.78	315	5480
1.87	310	5400
1.91	308	5360
2.02	312	5430
2.03	305	5310

(1) A total flow rate of 0.050 lb/sec was maintained.

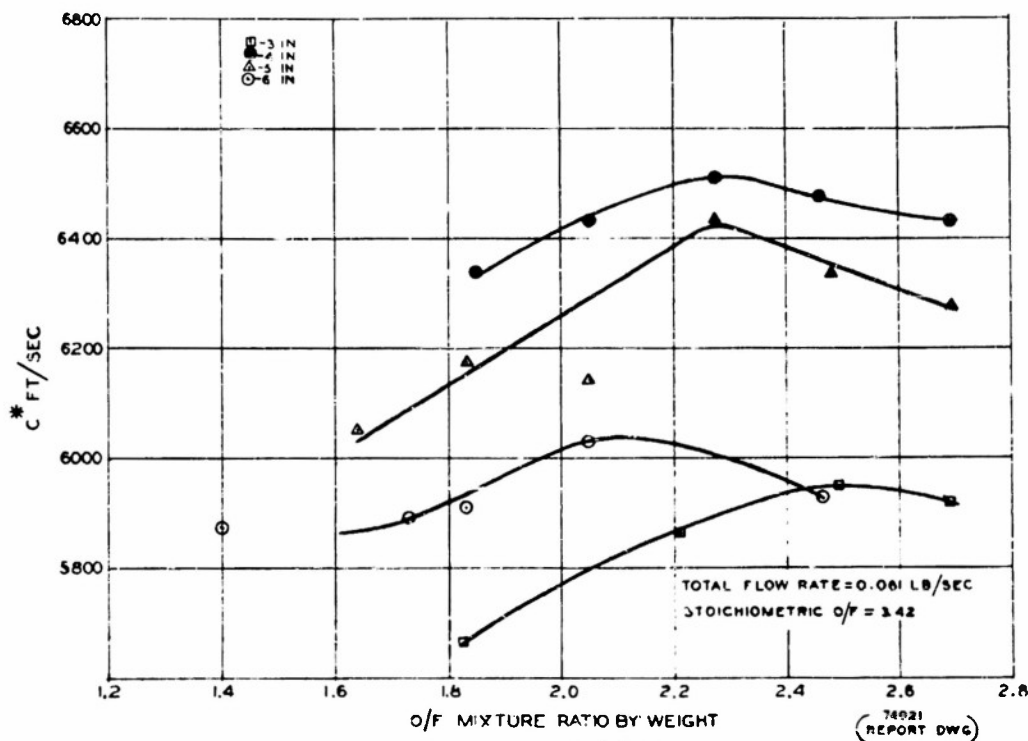


FIGURE 12  
CHARACTERISTIC VELOCITY VS MIXTURE RATIO  
ETHYLENE—LIQUID OXYGEN

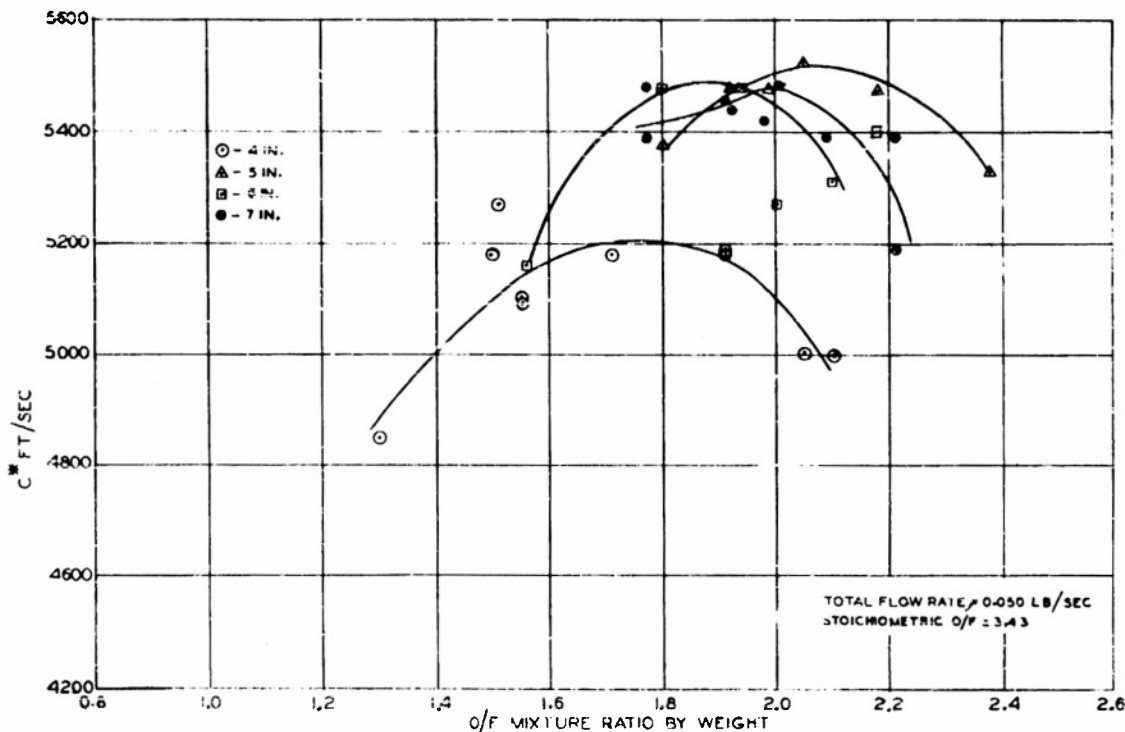


FIGURE 13  
CHARACTERISTIC VELOCITY VS MIXTURE RATIO  
CYCLOPROPANE—LIQUID OXYGEN

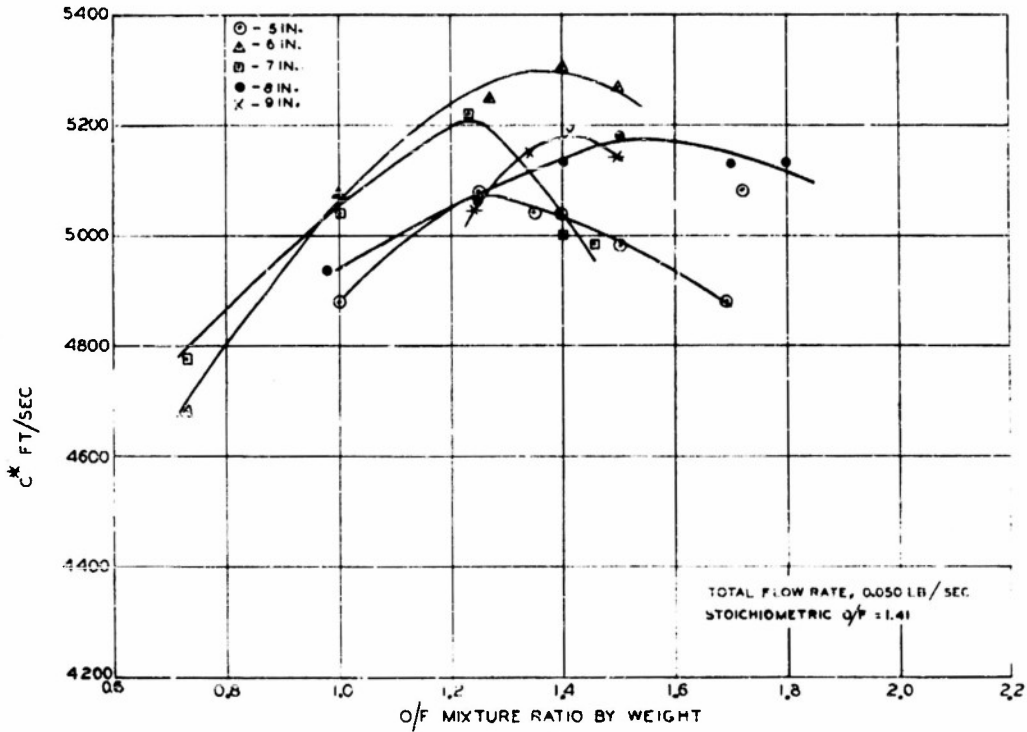


FIGURE 14  
CHARACTERISTIC VELOCITY VS MIXTURE RATIO  
AMMONIA-LIQUID OXYGEN

73886  
(REPORT DWG) 487

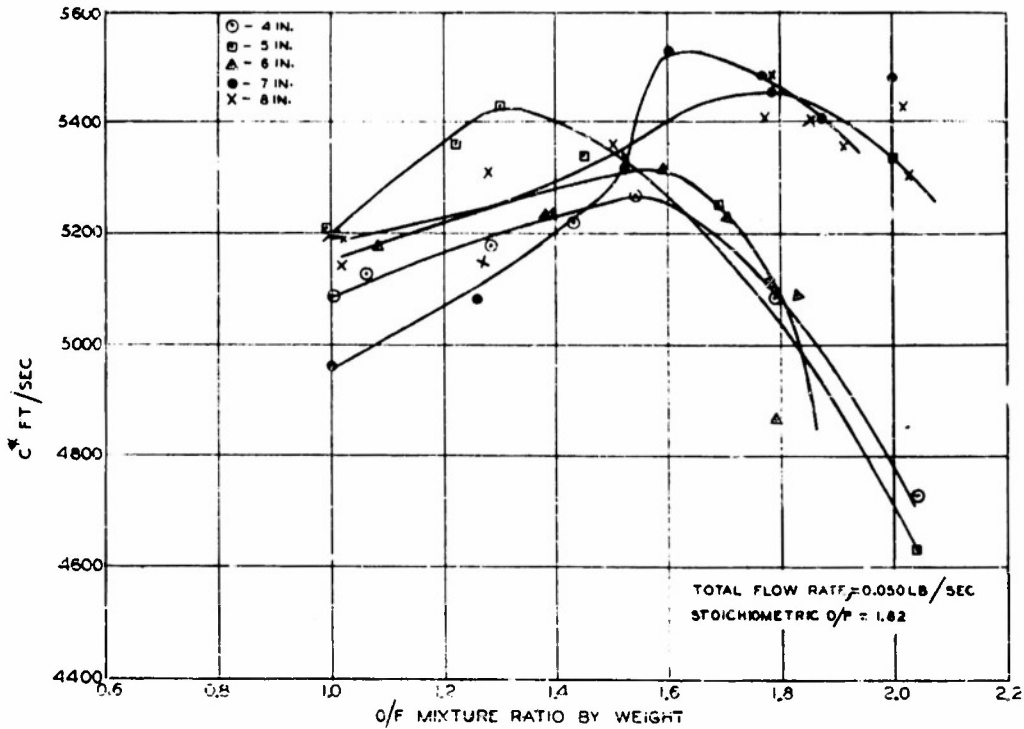


FIGURE 15  
CHARACTERISTIC VELOCITY VS MIXTURE RATIO  
ETHYLENE OXIDE-LIQUID OXYGEN

73887  
(REPORT DWG) 487

Maximum  $C^*$  values for ethylene, cyclopropane, ammonia, and ethylene oxide have been obtained at various chamber lengths from the graphs presented above. The chamber length for optimum performance for each of the fuel systems is determined from Fig. 16 which is a graph of maximum  $C^*$  as a function of chamber length. From this graph it is interesting to note that for ethylene the chamber length for optimum performance is four inches,  $C^* = 6510$  ft/sec at  $O/F = 2.27$ ; for cyclopropane it is five inches,  $C^* = 5530$  ft/sec at  $O/F = 2.05$ ; for ammonia it is six inches,  $C^* = 5310$  ft/sec at  $O/F = 1.40$ ; and for ethylene oxide it is seven inches,  $C^* = 5520$  ft/sec at  $O/F = 1.60$ .

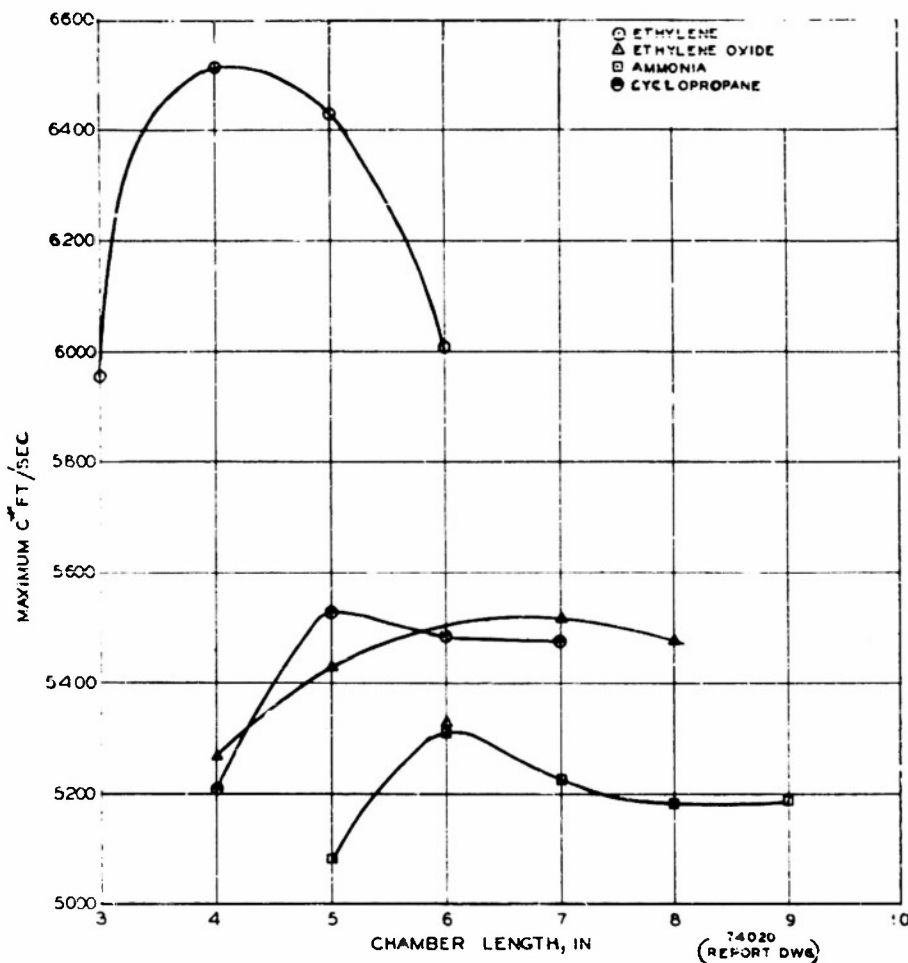


FIGURE 16  
MAXIMUM  $C^*$  OBTAINED EXPERIMENTALLY VS CHAMBER LENGTH

Figure 17 is a plot of theoretical  $C^*$  values at various mixture ratios by weight as reported by Brinkley, Smith and Edwards (Ref. 5). Their results are tabulated in Appendix A. The maximum theoretical  $C^*$  values from these curves may be compared with the experimental  $C^*$  values at various chamber lengths. Figure 18 shows a plot of the percentages of maximum theoretical  $C^*$  which were obtained experimentally as a function of chamber length. From these curves, the decreasing order of efficiency is ethylene (108.0%), ethylene oxide (96.6%), cyclopropane (92.6%), and ammonia (89.9%). In obtaining the efficiency values, duplicate runs have been made for the ethylene oxide, cyclopropane, and ammonia systems with liquid oxygen as the oxidizer. The efficiency for the ethylene-liquid oxygen system reported above is the result of a single determination at each O/F since time and funds prevented the carrying out of duplicate runs.

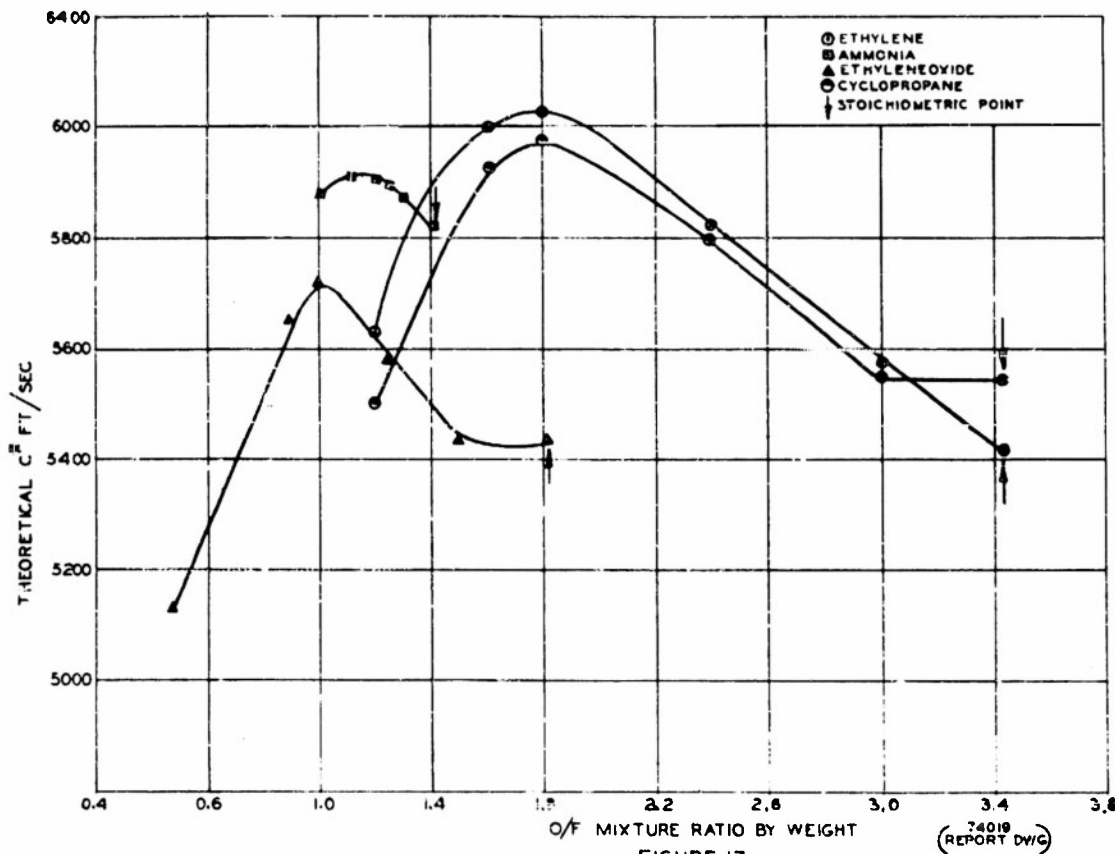


FIGURE 17  
THEORETICAL  $C^*$  VS MIXTURE RATIO

(74019 REPORT DWG)

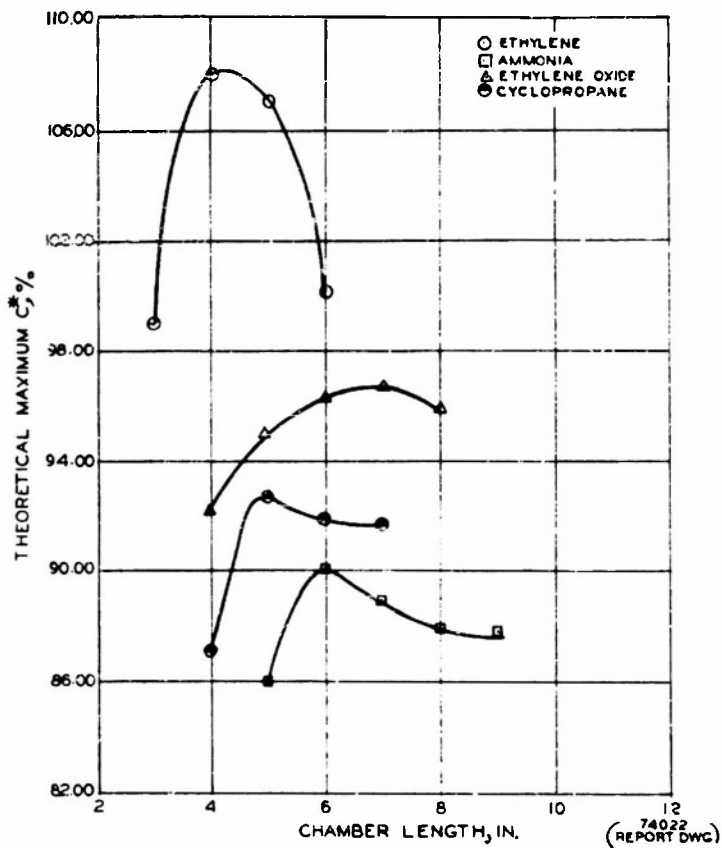


FIGURE 18 \*  
 PERCENT THEORETICAL MAXIMUM C OBTAINED  
 EXPERIMENTALLY VS CHAMBER LENGTH

6. CORRELATION OF DATA

Flame speed, slow oxidation, and small scale motor studies on ethane, ethanol, acetaldehyde, and ethylamine with an appropriate oxidant have been carried out at Reaction Motors, Inc. (Ref. 1). As a result of these studies, two empirical linear relationships were postulated. These were

$$V_a = -\frac{2.09}{m} + 4.68 \quad (2)$$

and

$$\log \frac{1}{m} = (0.200 \times 10^{-4}) \frac{V}{W^3} - 1.472 \quad (3)$$

where  $V_a$  = maximum apparent flame speed, ft/sec.

$m$  = slope of the plot of percent  $\text{CO}_2$  evolved vs the logarithm of the contact time from slow oxidation studies.

$V$  = combustion chamber volume of the motor, cu in.

$W$  = total flow rate of propellants, lb/sec.

The data which were used to obtain relationships (2) and (3) above are summarized in Table 7 together with data obtained in this study.

If the  $1/m$  value for ethylene is substituted in relationship (2), one obtains a value of 4.11 ft/sec. for the maximum apparent flame speed,  $V_a$ , of the ethylene-air system. This does not compare favorably with the experimental value of 5.53 ft/sec. In Ref. 1, a plot of the maximum apparent flame speed in ft/sec vs  $1/m$  has been drawn for the above four fuels. The pertinent data for the latter and ethylene have been replotted

TABLE 7  
SUMMARY OF DATA

Fuel	Max. Apparent Flame Speed $V_a$ , ft/sec	Chamber Length For Max. $C^*$ , L, in.	Chamber Volume (a) V, cu in.	Total Flow Rate, W, lb/sec	$\frac{V}{W^3} \times 10^{-4}$	Slope of Slow Oxidation Curve at 350°C, m	$\frac{1}{m}$
Ethanol (b)	4.32	4.0	5.69	0.0584	2.86	7.32	0.138
Acetaldehyde (b)	4.32	3.5	5.07	0.0509	4.06	5.03	0.199
Ethane (b)	3.79	9.0	11.84	0.0606	5.32	2.27	0.440
Ethylamine (b)	2.76	7.0	9.38	0.0500	7.50	1.10	0.912
Ethylene (c)	5.53	4.0	5.69	0.061	2.51	1.91	0.524
Ethylene Oxide (c)	8.73	7.0	9.38	0.050	7.50	— (d)	— (d)
Cyclopropane (c)	3.56	5.0	6.92	0.050	5.54	— (d)	— (d)
Ammonia (c)	— (e)	6.0	8.15	0.050	6.52	— (f)	— (f)

(a) Volume includes chamber and convergent section of nozzle.

(b) Data are taken from Report RMI 442-F.

(c) Data have been obtained under this contract.

(d) When plotted, the data from these fuels did not yield straight lines.

(e) Datum is not available.

(f) This fuel is not applicable to current slow oxidation studies.

in Fig. 19. It is seen that the point for ethylene does not fall on the curve drawn through the points for the other fuels.

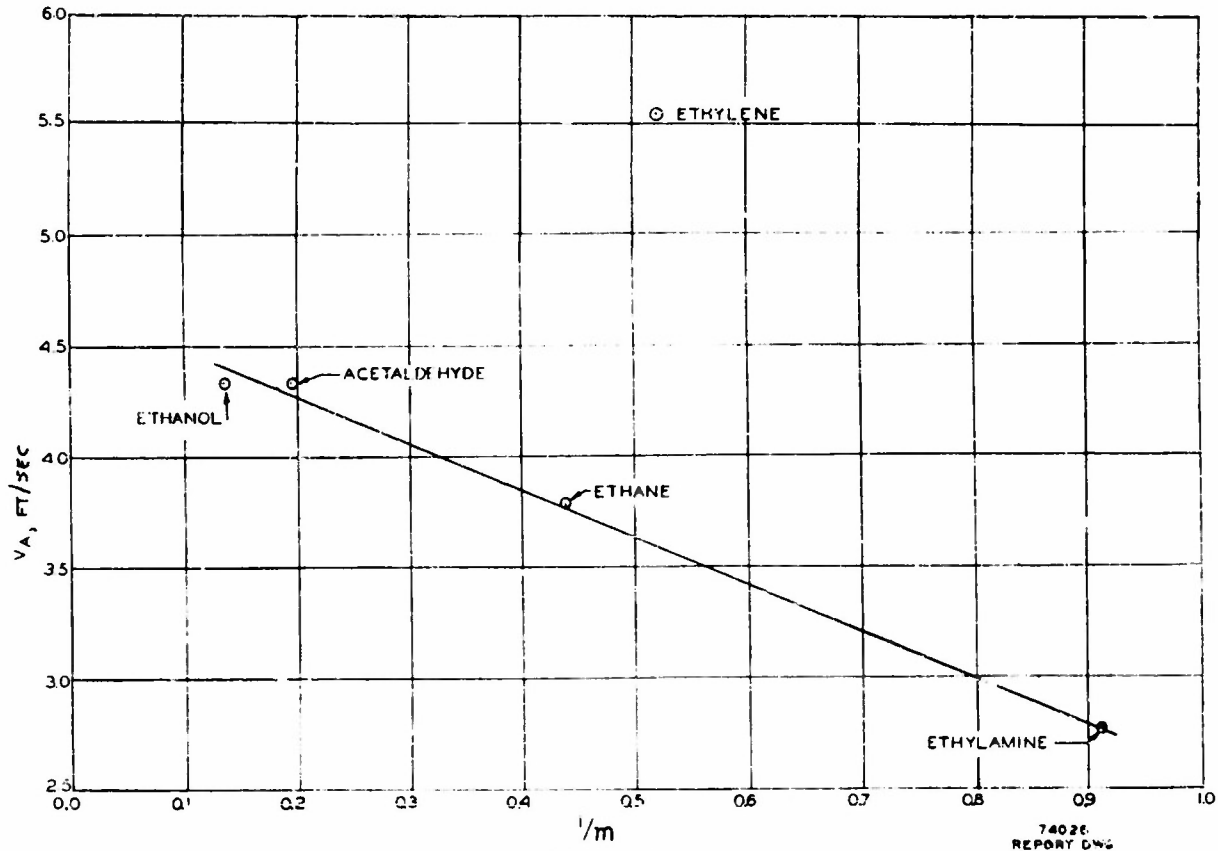


FIGURE 19  
MAXIMUM APPARENT FLAME SPEED VS  $1/m$   
( $m$  IS SLOPE OF THE PLOT OF THE %  $CO_2$  EVOLVED  
VS LOG CONTACT TIME - FIG. 6)

Utilizing the  $V/W^3$  value for ethylene from Table 7 and substituting in relationship (3) one obtains a value of 0.113 for  $1/m$ . This again does not agree favorably with the experimental value of 0.524 for  $1/m$  for ethylene. In Ref. 1,  $1/m$  has been plotted against  $V/W^3$  for the same four fuels. These points have been replotted in Fig. 20, together with the point for ethylene. Once again the latter does not fall on the curve drawn through the four points.

The above considerations show that ethylene does not satisfy the postulated relationships (2) and (3).

Slow oxidation studies on the ethylene oxide-oxygen and cyclopropane-oxygen systems yielded no linear relationships between the percent  $\text{CO}_2$  and the logarithm of the contact time (Fig. 6). Since  $m$ , the slope of the plot of percent  $\text{CO}_2$  vs the logarithm of the contact time, is involved in relationships (2) and (3), studies on these two systems further invalidate relationships (2) and (3).

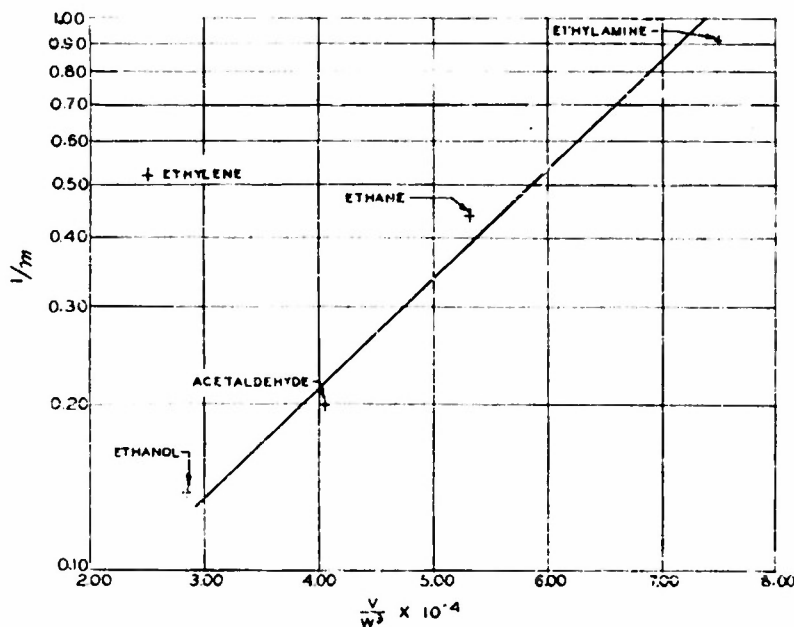


FIGURE 20  
RELATIONSHIP AMONG CHAMBER VOLUME, FLOW RATE, AND  $1/m$

## 7. CONCLUSIONS

As a result of flame speed, slow oxidation, and small scale rocket motor studies on the systems ethylene, cyclopropane, ethylene oxide, and ammonia with appropriate oxidants, the following conclusions may be drawn:

1. The maximum apparent flame speeds for ethylene oxide, ethylene, and cyclopropane with air as the oxidant were found to be 266, 169, and 109 cm/sec, respectively.
2. Slow oxidation studies on the cyclopropane-oxygen system at 350°C yielded no measurable amount of CO<sub>2</sub>.
3. Slow oxidation studies in the ethylene oxide - oxygen system at 350°C resulted in a decrease in percent CO<sub>2</sub> with increase in contact time.
4. A linear relationship is indicated between the percent CO<sub>2</sub> and the logarithm of the contact time for the ethylene-oxygen system at 350°C with an induction period of 79 sec.
5. Experimental determinations of optimum performance employing C\* in ft/sec as the performance parameter, at the minimum chamber length (volume) showed the following decreasing order for the fuel-lox systems: ethylene, 6510 (4 in. chamber); cyclopropane, 5530 (5 in. chamber); ethylene oxide, 5520 (7 in. chamber); and ammonia, 5310 (6 in. chamber).
6. The data for the ethylene-oxidant system do not satisfy the linear relationships proposed in Ref. 1.
7. The data for the ethylene oxide-oxidant and the cyclopropane-oxidant systems do not satisfy the linear relationships proposed in Ref. 1.

## 8. RECOMMENDATIONS

As a result of the studies undertaken under this contract, the relationships postulated in Ref. 1 were shown to be invalid. In view of this fact, the following recommendations are made:

1. Research in the field of combustion phenomena with the goal of finding a correlation among flame speed, oxidation processes, and small scale rocket motor characteristics should be continued.
2. Laboratory flame speed and slow oxidation studies under the conditions indicated in this and in the previous report (Ref. 1) should be discontinued.
3. Inasmuch as wall effects unquestionably play a major role in combustion phenomena, the flame speed and slow oxidation equipment should be redesigned so that wall effects will be common in all three operations.
4. Since the validity of utilizing data obtained from temperature reactions for possible correlations with very high temperature data obtained from rocket motor studies is gravely doubtful, the three operations should be carried out at temperatures which are of the same order of magnitude.
5. The small scale motor and injector should be redesigned to facilitate changes in chamber length, flow rate, and O/F ratios during actual motor operations. This will result in a saving of time and in facilitating duplication of runs.

CONFIDENTIAL

Reaction Motors, Inc.

Report RMI-487-F

REFERENCES

1. Reaction Motors, Inc., Report RMI-442-F, "Investigation of Chemical Combustion Kinetics", Contract AF 33(038)-23176.
2. B. Lewis and G. von Elbe, "Combustion, Flames and Explosions of Gases" pp. 749-751, Academic Press, Inc., New York, New York, 1951.
3. E. R. Stephens and R. N. Pease, J. Am. Chem. Soc., 72, 1188 (1950).
4. R. White, J. Chem. Soc., 121, 1688 (1922).
5. S. R. Brinkley, Jr., R. W. Smith, Jr., and H. E. Edwards, "Thermodynamics of the Combustion Products of Some Fuel-Liquid Oxygen Systems", Bureau of Mines Report PX3-107/15, September 1953.

## APPENDIX A

## THEORETICAL PERFORMANCE PARAMETERS

FOR

VARIOUS FUEL - LIQUID OXYGEN SYSTEMS AT A CHAMBER  
 PRESSURE OF 300 PSIA AND AN EXHAUST PRESSURE OF 1 ATMOSPHERE  
 FROZEN EQUILIBRIUM METHOD\*

## CYCLOPROPANE-LIQUID OXYGEN

O/F (b. w.)	1.20	1.60	1.80	2.40	3.00	3.43**
Flame Temp. (°K)	2315.2	3071.9	3290.9	3467.1	3408.9	3582.3
Exhaust Temp. (°K)	1113.3	1601.0	1752.5	1900.7	1885.6	2044.6
$\gamma = C_p/C_v$	1.2967	1.2618	1.2513	1.2386	1.2336	1.2209
$C^*$ (ft/sec)	5499.2	5924.2	5971.8	5795.6	5545.8	5542.1
$t_{sp}$ (sec)	236.67	256.69	259.11	252.05	241.32	241.71

## ETHYLENE-LIQUID OXYGEN

O/F (b. w.)	1.20	1.60	1.80	2.40	3.00	3.42**
Flame Temp. (°K)	2423.0	3136.0	3336.5	3491.5	3430.7	3373.5
Exhaust Temp. (°K)	1176.2	1634.5	1774.6	1909.4	1893.3	1868.9
$\gamma = C_p/C_v$	1.2947	1.2618	1.2521	1.2399	1.2349	1.2326
$C^*$ (ft/sec)	5630.2	5995.2	6024.7	5828.9	5574.5	5421.8
$t_{sp}$ (sec)	242.43	259.74	261.34	253.45	242.50	235.96

## AMMONIA-LIQUID OXYGEN

O/F (b. w.)	1.00	1.10	1.20	1.25	1.30	1.41**
Flame Temp. (°K)	2778.7	2929.3	3029.5	3061.5	3083.0	3102.6
Exhaust Temp. (°K)	1550.5	1657.7	1731.5	1755.4	1772.7	1788.5
$\gamma = C_p/C_v$	1.2242	1.2191	1.2158	1.2146	1.2135	1.2122
$C^*$ (ft/sec)	5869.9	5910.5	5908.6	5894.5	5873.9	5812.3
$t_{sp}$ (sec)	255.74	257.89	258.09	257.59	256.72	254.07

## ETHYLENE OXIDE-LIQUID OXYGEN

O/F (b. w.)	0.50	0.75	1.00	1.25	1.50	1.82**
Flame Temp. (°K)	2170.7	2953.8	3300.5	3341.5	3309.4	3508.2
Exhaust Temp. (°K)	1062.9	1565.7	1813.1	1858.0	1849.5	2027.5
$\gamma = C_p/C_v$	1.2881	1.2526	1.2363	1.2308	1.2282	1.2144
$C^*$ (ft/sec)	5156.8	5651.9	5713.1	5581.2	5432.5	5430.8
$t_{sp}$ (sec)	222.19	245.24	248.51	242.99	236.63	237.13

\*These values are taken from Ref. 5.

\*\*Stoichiometric ratio.